

# On the Diurnal, Annual, and Solar Cycle Variations of Slant Total Electron Content in the Korean Peninsula

Woong-Jun Yoon<sup>1†</sup>, Kwan-Dong Park<sup>2</sup>

<sup>1</sup>Department of Geoinformatic Engineering, Inha University, 100 Inha-ro, Nam-gu, Incheon 22212, Korea

<sup>2</sup>Jipyong Space Inc., #39-307, 100 Inha-ro, Nam-gu, Incheon 22212, Korea

## ABSTRACT

The ionospheric error, which is one of many error elements considered during the Global Navigation Satellite System (GNSS) positioning, is hard to be predicted due to the influence of geomagnetic activity and irregular solar activities. Thus, the present study analyzed a change pattern in the ionosphere through Global Ionosphere Map (GIM) data for 12 years from 2003 to 2014 and a variation in the Slant Total Electron Content (STEC) between Sinuiju and Busan which was the longest range in the southeastern direction of the Korean Peninsula. The variation in the STEC verified the diurnal, annual, and solar cycle variations due to the influence of solar activity. The diurnal variation was characterized that the variation in the STEC started to increase from 6–7 am and reached the maximum at 13–14 pm followed by being decreased. The seasonal variation was characterized that the variation in the STEC was high in spring and autumn whereas it was low in summer and winter. The solar cycle variation revealed that the variation in the STEC increased during solar maximum and decreased during solar minimum. The variation in the STEC was up to 20 Total Electron Content Unit (TECU) during the solar minimum and up to 60 TECU during solar maximum.

**Keywords:** STEC, diurnal, annual, solar cycle

## 1. INTRODUCTION

The Global Navigation Satellite System (GNSS) was developed initially for military purpose but it was allowed to be used in private purpose since 1996 thereby being utilized in many fields including not only military purpose but also vehicle, ships, and airplanes. Positioning using the GNSS includes a number of errors, which were caused by ionospheric delay, tropospheric delay, multi-path error, and clock errors. In recent years, a large number of studies on reduction in error within 1m distance during positioning via a low-price single receiver. The ionospheric error among

them is about 5–15m at day time and 1–3m at night in the mid-latitude region on the basis of the zenith direction. This error is very difficult to be predicted because of the influence of solar and geomagnetic activities (Misra & Enge 2011).

The ionosphere reflects or refracts radio waves from extraterrestrial sources thereby creating an ionospheric error when GNSS signals are passed through the ionosphere. The ionospheric delay error can be eliminated up to 99% using a difference in refraction rate between L1 and L2 signals (Hofmann-Wellenhof et al. 2008). However, it is difficult to ensure high accuracy of positioning for low-price receivers that use a single frequency due to the ionospheric delay error.

The relative positioning such as Differential Global Positioning System or Real Time Kinematic (RTK), which are much utilized in recent years, can minimize various errors including the ionospheric delay error by receiving correction information from the reference station even with

---

Received April 11, 2016 Revised May 09, 2016 Accepted May 12, 2016

<sup>†</sup>Corresponding Author

E-mail: yoongoodid@naver.com

Tel: +82-32-873-4305 Fax: +82-2-6455-4305

single frequency receivers thereby ensuring accuracy of 1–3 m in the case of DGPS and 1–3 cm in the case of RTK. The DGPS creates the Pseudo Range Correction (PRC) including the correction of ionospheric delay error at the reference station, which knows the precise positioning, and then transfers the created PRC to the user thereby correcting the user positioning error. The RTK can provide high positioning accuracy by offsetting a common error of user and the reference station which knows the precise position during positioning using a carrier wave. However, as a distance between user and reference station becomes farther, the ionospheric error in the common error components varies so that a single frequency receiver is limited to relative positioning of long baseline (Kang et al. 1996).

Thus, the present study aimed to determine the effect of the ionospheric error on positioning during long baseline relative positioning using a single frequency quantitatively and analyzed the maximum of the variation in the Slant Total Electron Content (STEC) between Busan and Sinuiju, which is the longest line (675 km) in the southeastern direction in the Korean Peninsula for a long term from 2003 to 2014 to identify the change in the ionosphere. For the comparison of the ionosphere between Busan and Sinuiju, Vertical Total Electron Content (VTEC) values in the corresponding region provided through the Global Ionosphere Map (GIM) model were used and converted to STEC values that were used in real positioning thereby analyzing the variations in STEC and periodicity due to the diurnal, annual, and solar cycle variations.

## 2. TYPES OF THE IONOSPHERE MODEL

A type of the ionosphere model that is used to correct the ionospheric delay error is various according to the use purpose and analysis method. Among them, Klobuchar model, International Reference Ionosphere (IRI) model, and GIM model are widely used in the GNSS (Choi 2009). Each of the models has different use methods and error correction rate. Although the Klobuchar model can be used in real time positioning, its correction rate is just 50–60%. On the other hand, a correction rate of the IRI model is higher than that of the Klobuchar model but it is not used in real time positioning because it is an empirical model. As such, an optimum model among the ionospheric models shall be selected depending on positioning circumstance.

### 2.1 Klobuchar Model

The Klobuchar model estimates total electron content

in the ionosphere approximately using ION alpha and ION beta coefficients transferred from a GPS navigation system by users who use single frequency receivers. It can correct errors up to 50%–60% (Klobuchar 1987). This model sets the ION alpha and ION beta coefficients considering the observation date and a mean sun flux at the central control station and calculates the total electron content in the ionosphere assuming that electrons are concentrated at a virtual layer whose thickness is 0 at an altitude of 350 km using the coefficients. A unit of electron contents is Total Electron Content Unit (TECU). One TECU means that there are  $1 \times 10^{16}$  electrons at a column whose base area is 1 m<sup>2</sup>. It is assumed that the TEC in the ionosphere calculated through the Klobuchar model is highest at 14 pm and constant as 9.24 TECU between 22 pm and 06 am (Klobuchar 1987).

### 2.2 IRI Model

The IRI model is an empirical ionospheric model based on past data, which can calculate not only TEC in the ionosphere but also ion composition and temperature using various equations and 100 or more parameters according to conditions (Choi 2009). The IRI model is provided via the FORTRAN code and user-preferred date, time, latitude, longitude, and altitude are used as input variables thereby calculating the TEC inside the ionosphere up to 50–2000 km. The IRI model is updated consistently through research and improvement and the most-up-to-date version is IRI-2012, which can correct errors up to 75% (Choi 2009).

### 2.3 GIM Model

The GIM is a map that shows the TEC inside the ionosphere around the earth, which is provided by the International GNSS Service (IGS). It is created using base functions such as triangular grid interpolation and spherical harmonics by collecting information obtained from 1 hundred or more observatories around the world. The GIM model provides a value in the grid whose size is latitude 2.5° and longitude 5° via the IONEX format and data are updated in every two hour (Schaer et al. 1998). The GIM model provides only VTEC so it is needed to be changed to STEC by using obliquity factor when it is used in the GNSS positioning. In this study, the GIM model was selected to analyze ionospheric information accurately among the Klobuchar model, IRI model, and GIM model because it had the highest correction rate (Choi 2009).

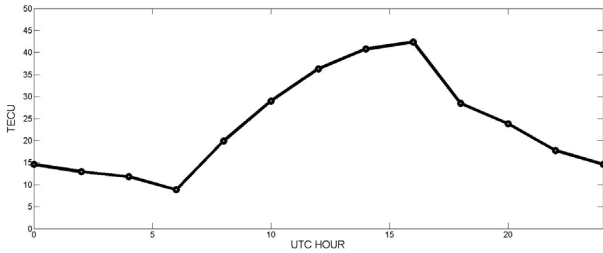


Fig. 1. Changes in electron contents at January 1 2014.

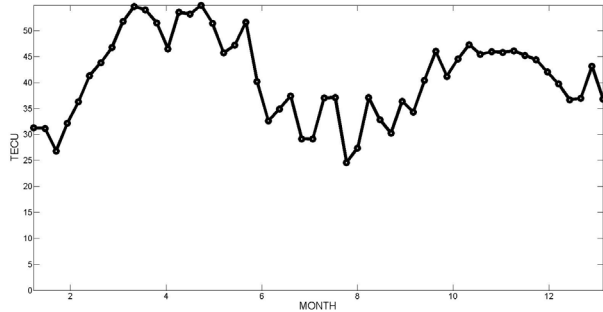


Fig. 2. Variation in electron contents between January and December in 2014.

### 3. CYCLE OF THE IONOSPHERE VARIATION

Prior to analyzing the trend of deviation in the STEC in the Korean peninsula, periodicity of the GIM mode was analyzed according to the diurnal, annual, and solar cycle variations in order to determine the characteristics of the GIM model. The solar meridian altitude, season, and solar cycle change the intensity of solar radiation that affects the ionosphere and variations in TEC values that are provided by the GIM model show periodicity due to the periodical change. In order to verify the periodicity, a cycle of variation in the TEC was checked at an arbitrary user location (latitude 30° and longitude 0°) using the GIM model from 2003 to 2014. A unit of the ionosphere in the GIM model provided in every two hour was converted to TECU.

Fig. 1 shows the GIM model data at the user location (latitude 30°, longitude 0°) for 24 hours from UTC 00:00 to 24:00 of January 1 in 2014. As shown in Fig. 1, a change in the ionosphere in a day was the lowest at 6 am as 9 TECU and electron content was increased rapidly from 6 to 7 am when the sun rose and reached the highest as 42 TECU at 13 to 14 pm. This result means that solar radiation on the atmosphere is increased as the solar meridian altitude is higher and then as the solar meridian altitude is lower, electron content is also reduced.

Fig. 2 shows the GIM model data as a weekly mean value for one year from January to December in 2014 in order to analyze

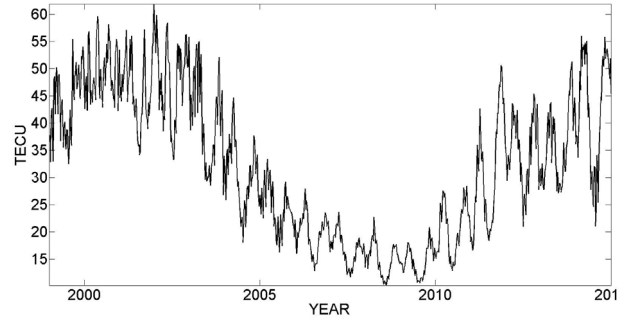


Fig. 3. Change in TEC from 1998 to 2014.

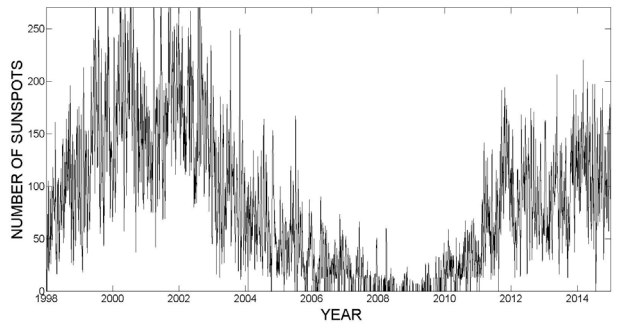


Fig. 4. Change in the number of sunspots yearly (NASA Solar cycle prediction 2016).

a seasonal change in the ionosphere. The TEC was the highest as about 50 TECU in April and May in spring and reduced to about 30 TECU in July and August in summer. It was increased to about 45 TECU in October and November in autumn and then reduced to about 30 TECU in December and January in winter. Due to the characteristic of the ionosphere which was affected much by solar activities, the highest TEC was expected during summer but the highest TEC was revealed during spring and autumn on the contrary. This result was consistent with the monthly periodicity of the TEC in the ionosphere observed in regular observatories in Cheorwon, Suwon, and Jeju using the Klobuchar model in 2009 (Lee et al. 2010). The same periodicity was also found in the GIM model. The reason for this was not clearly disclosed yet but there was a study on suppression of ionization in the ionosphere as free electrons moved along the magnetic field lines in the earth from the northern to southern hemisphere during the summer in the northern hemisphere whereas free electrons moved from the southern to northern hemisphere during the summer in the southern hemisphere (Rishbeth 1972).

The solar magnetic activity is a periodic 11-year change and the cycle can be found via various phenomena such as change in the number of sunspots and solar flare. Fig. 3 shows the weekly mean value of the ionosphere at the aforementioned user location calculated using the GIM model thereby showing a time-series change for 16 years from 1999 to 2014. Fig. 4 shows a graph of the solar cycle

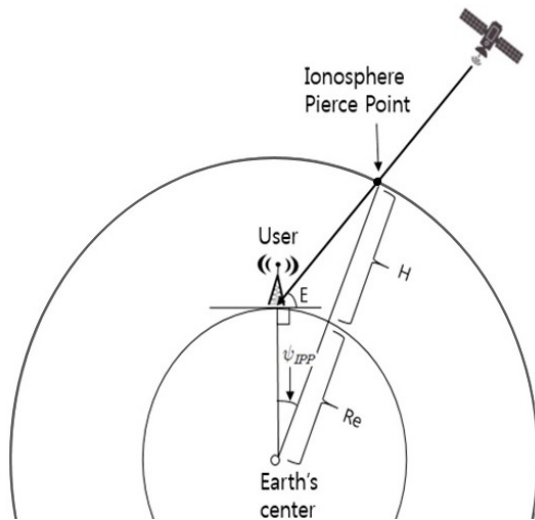


Fig. 5. Geometrical diagram of the IPP.

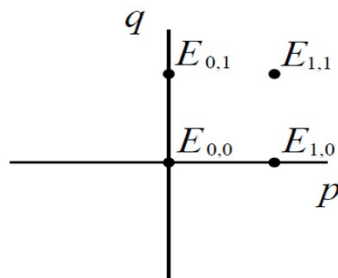


Fig. 6. Configuration of the grid in the IONEX interpolation.

prediction provided by the NASA, which predicted the change in the number of sunspots by year from 1985 to 2020. These two graphs from 1999 to 2014 show a very similar pattern (NASA Solar cycle prediction 2016). Thus, we can infer that the number of sunspots is closely related to the TEC in the ionosphere. At the solar maximum from 2002 to 2003 where the number of sunspots was increased, a mean value of the ionosphere was increased to around 50 TECU and a mean value of the ionosphere was decreased to around 12 TECU at the solar minimum in 2008.

#### 4. METHOD OF ANALYSIS ON STEC VARIATION

Relative positioning such as DGPS and RTK is highly accurate within an error of 1 m and 1 cm, respectively (Kim et al. 2012). However, relative positioning has a shortcoming that positioning error is increased as a baseline distance between reference station and user becomes farther. A STEC variation between reference station and user, which is one of the relative positioning error components, is

affected not only by the baseline distance but also by solar elevation angle, seasons, and solar magnetic activities. Accordingly, we selected Sinuiju and Busan as comparison locations, which produced the longest baseline in the southeastern direction in the Korean Peninsula, thereby studying the change and periodicity of STEC variation by the diurnal, annual, and solar cycle variations. The latitude and longitude of Busan and Sinuiju are 35.15 N and 129.05 E and 40.10 N and 124.40 E. For ionospheric data, GIM data provided by the IGS were employed, which were obtained for 12 years from 2003 to 2014. Since the GIM data provided  $2.5^\circ \times 5^\circ$  latitude-longitude VTEC grid data in every two hour, the data were converted to STEC for each satellite. Fig. 5 shows the geometrical characteristics of Ionosphere Pierce Point (IPP) between satellite and user location, in which the IPP is a location where the satellite signal is passed through the virtual ionospheric band whose altitude is 350 km and thickness is 0.  $\varphi$  and  $\lambda$  refer to a latitude and a longitude to represent user location  $(\varphi_{user}, \lambda_{user})$  and IPP location  $(\varphi_{IPP}, \lambda_{IPP})$ ,  $E$  refers to an elevation angle of satellite,  $R_e$  is a radius of the earth (6378.137 km),  $H$  refers to an altitude of the IPP (350 km),  $\psi_{IPP}$  refers to an angle between user location and IPP from the center of the earth, and  $A$  refers to an azimuth of the satellite. Eq. (1) calculates an angle between user location and IPP from the center of the earth and Eq. (2) calculates latitude of the IPP, and Eq. (3) calculates a longitude of the IPP (Klobuchar 1987).

$$\psi_{IPP} = \frac{\pi}{2} - E - \sin^{-1}\left(\frac{R_e}{R_e+H} \cos E\right) \tag{1}$$

$$\varphi_{IPP} = \sin^{-1}(\sin \varphi_{user} \cos \psi_{IPP} + \cos \varphi_{user} \sin \psi_{IPP} \cos A) \tag{2}$$

$$\lambda_{IPP} = \lambda_{user} + \sin^{-1}\left(\frac{\sin \psi_{IPP} \sin A}{\cos \varphi_{IPP}}\right) \tag{3}$$

In the VTEC value at the calculated IPP location, interpolation was performed using an interpolation method (Eq. 4) proposed by the IONEX with surrounding four grid points given at the GIM data. After selecting four surrounding grid points at the IPP latitude and longitude, VTEC was calculated at the IPP based on the VTEC in the four grid points. In Eq. (4),  $q$  and  $p$  refer to  $y$  and  $x$  values in the grid as shown in Fig. 6 and current user location  $E$  is distanced away from  $E_{0,0}$  as much as  $\Delta\lambda$  by latitude and  $\Delta\beta$  by longitude. The VTEC shall be converted to STEC for each satellite using a Mapping Function in order to be used in real positioning. In this study, the VTEC was converted to STEC in order to analyze the ionospheric error that affected positioning. A Mapping Function (MF) is shown in Eq. (5) and a method of conversion of VTEC to STEC is shown in Eq. (6) (Sohn 2015).

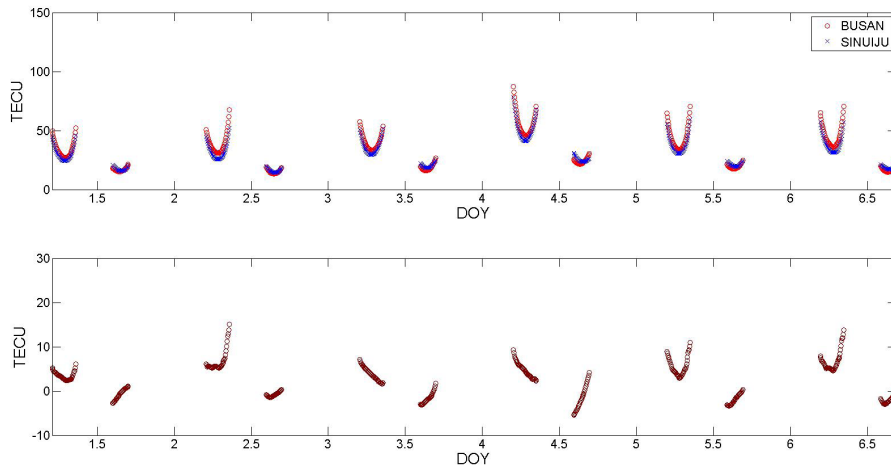


Fig. 7. STEC variation (upper) and difference (lower) between Busan and Sinuiju at DOY 1–6 and PRN No. 8 in 2003.

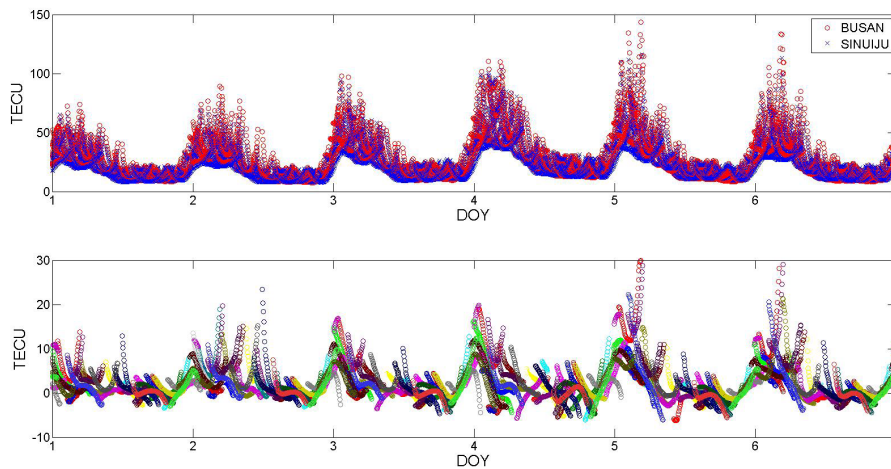


Fig. 8. STEC variation (upper) and difference (lower) between Busan and Sinuiju at DOY 1–6 and all satellites in 2003.

$$E(\lambda_0 + p\Delta\lambda, \beta + q\Delta\beta) = (1-p)(1-q)E_{0,0} + p(1-q)E_{1,0} + q(1-p)E_{0,1} + pqE_{1,1} \quad (4)$$

$$MF = \frac{1}{\sqrt{1 - \left(\frac{R_e}{R_e + H} \cos E\right)^2}} \quad (5)$$

$$\text{STEC} = MF \times \text{VTEC} \quad (6)$$

Eq. (5) was used to calculate STEC for each satellite in Busan and Sinuiju using the VTEC provided by the GIM data. The STEC was calculated only when a specific satellite was observed at the same time in Busan and Sinuiju and a difference in STEC between Busan and Sinuiju was calculated to analyze the STEC variation. The STEC variations according to diurnal, annual, and solar cycle were analyzed. Arbitrary six days in 2003 were selected and

analyzed for the diurnal analysis. For the annual analysis, six days in 2003 that corresponded to spring, summer, autumn, and winter were selected respectively thereby analyzing the change due to season. For the solar cycle analysis, solar maximum in 2003, solar minimum in 2008, and Day of Year (DOY) 141–146 during solar maximum in 2014 were selected to verify the effect of the 11-year solar magnetic activity cycle on the STEC variation.

## 5. RESULT AND DISCUSSION

The analysis results on STEC variation were as follows. Fig. 7 shows STEC values (upper) and STEC variations (lower) of DOY 1–6 and PRN No. 8 satellite at Busan and Sinuiju in 2003. During this period, PRN No. 8 satellite was

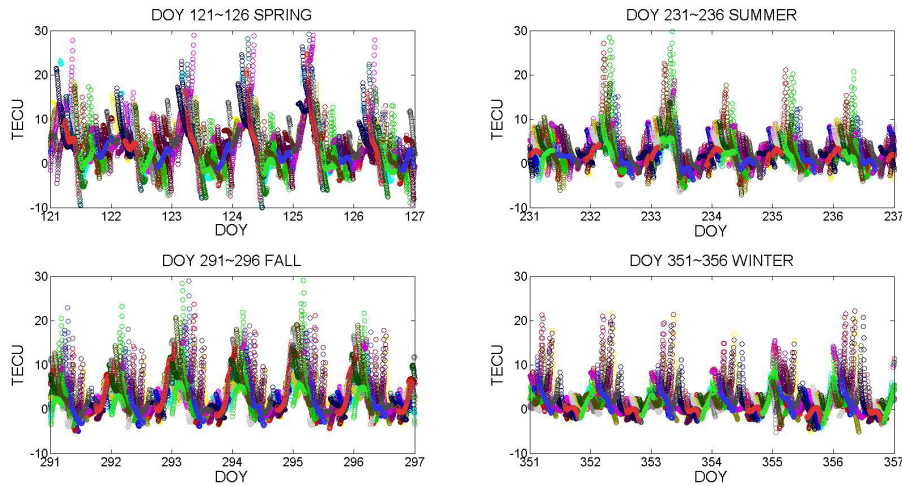


Fig. 9. Variation in STEC difference by season in 2003.

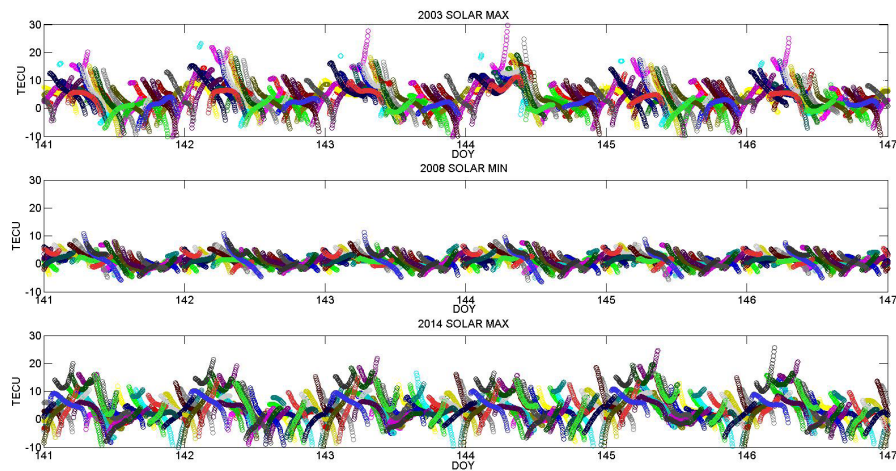


Fig. 10. Variation in the STEC difference between Busan and Sinuiju in 2003, 2008, and 2014.

observed twice a day. The STEC value was increased as an elevation angle was reduced when a satellite was descended. As an elevation angle is lower, a length where the satellite signal is passed through the ionosphere is longer thereby increasing the STEC value. Fig. 8 shows a collective graph of STECs of all satellites from PRN 1 to 32 in contrast with Fig. 7 showing only STEC value of a single satellite. It shows STEC values and STEC variations of all satellites from DOY 1-6 and PRN 1-32. A diurnal variation, which was not revealed in STEC value in a single satellite as shown in Fig. 7, can be clearly shown when diurnal variations from all PRNs were represented. From 6 to 7 am when the sun arose, the STEC variation, which was within a range of 0 and 5 TECU, started to increase and some variation exceeded 20 TECU at 13 to 14 pm. A pattern of variation was similar with that of VTEC which was large during the day but was small during the night.

The variation in STEC difference was also revealed clearly by season. Fig. 9 shows STEC differences during spring DOY 121-126 (upper left), summer DOY 231-236 (upper right), autumn DOY 291-296 (lower left), and winter DOY 351-356 (lower right) in order to see seasonal variation in 2003. Only a range of -5-30 was shown to see the variation in difference easily although there was a value over 30 TECU. In the spring, a variation in STEC difference was large indicating up to 60 TECU difference and a mean for six days was 4.77 TECU. In the summer, a variation in STEC difference was smaller than that in the spring as shown in the figure. In fact, a variation in STEC difference was reduced gradually as season moved from spring to summer. The STEC difference in summer was up to 30 TECU and a mean was 2.95 TECU. In the autumn, a variation of STEC difference was increased again and its difference was up to 32 TECU and a mean was 3.56 TECU. In the winter, the least variance

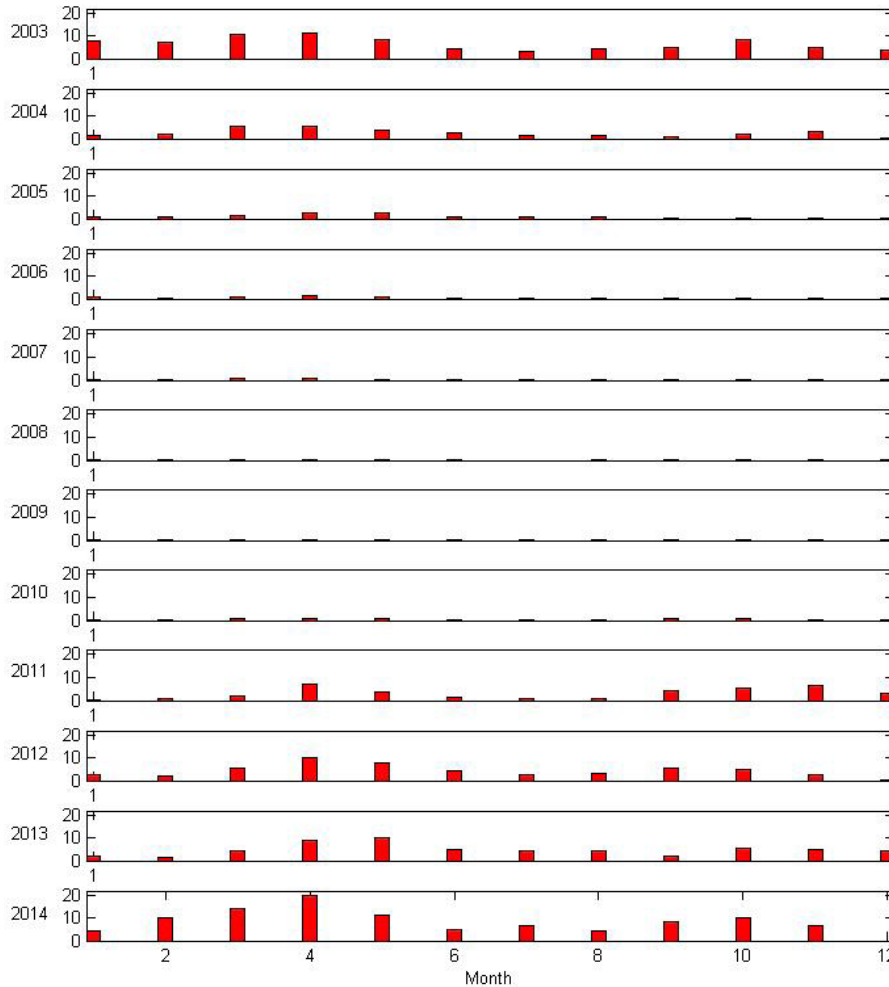


Fig. 11. Monthly relative frequency whose STEC difference was 10 TECU or larger.

in STEC difference was revealed among four seasons and its difference was up to 22 TECU and a mean was 2.23 TECU. The analysis result on seasonal variation revealed that the STEC difference between Busan and Sinuiju became larger during spring and autumn but it was smaller during summer and winter compared to that in the spring and autumn.

Fig. 10 shows the STEC difference of DOY 141-146 during solar maximum in 2003 (upper), solar minimum in 2008 (middle), and again solar maximum in 2014 (lower) in order to see the variation in STEC difference according to 11-year periodic solar magnetic activities. The STEC difference in 2003 during solar maximum was up to 40 TECU and a mean STEC for six days was 4.86 TECU. The STEC difference was reduced gradually as it went from the solar maximum to solar minimum and during solar minimum in 2008, the STEC difference was up to 11 TECU, indicating the variation was smaller. A mean of the STEC difference of DOY 141-146 in 2008 was 1.81 TECU. The STEC difference started

to increase again as it went from the solar minimum to solar maximum and during solar maximum in 2014, the STEC difference was up to 25 TECU and a mean was 4.63 TECU. Based on the above results, a variation in the STEC difference was closely related to the solar cycle.

In order to see the variation cycle of STEC difference between Busan and Sinuiju easily, values of STEC difference more than 10 TECU were collected thereby showing relative frequencies. Fig. 11 shows a ratio of monthly relative frequency whose STEC difference between Busan and Sinuiju was 10 or larger TECU from 2003 to 2014. The monthly ratio of 10 TECU or larger showed also variations according to annual and solar cycle as the same as shown in the above result. The relative frequency ratio was increased during spring and autumn and decreased during summer and winter. The relative frequency ratio was increased during solar maximum but decreased during solar minimum. During the spring of solar maximum, the ratio was up to 20%. During solar minimum, most relative

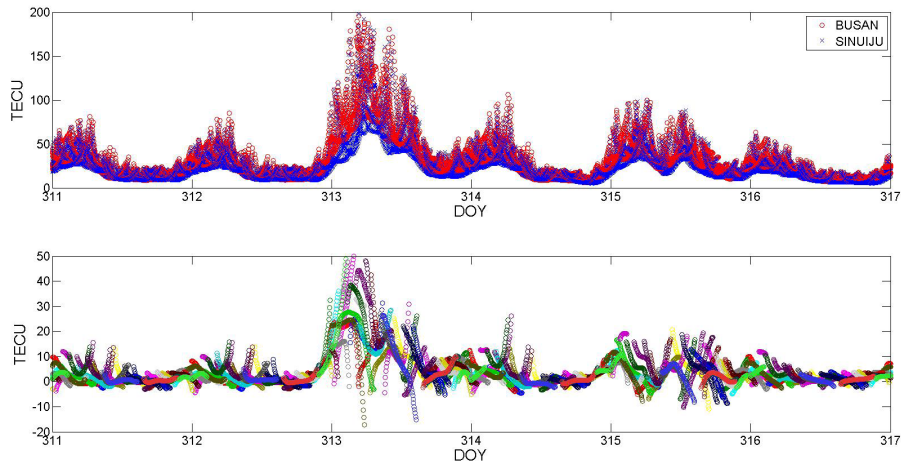


Fig. 12. STEC difference of DOY 311–316 in 2004.

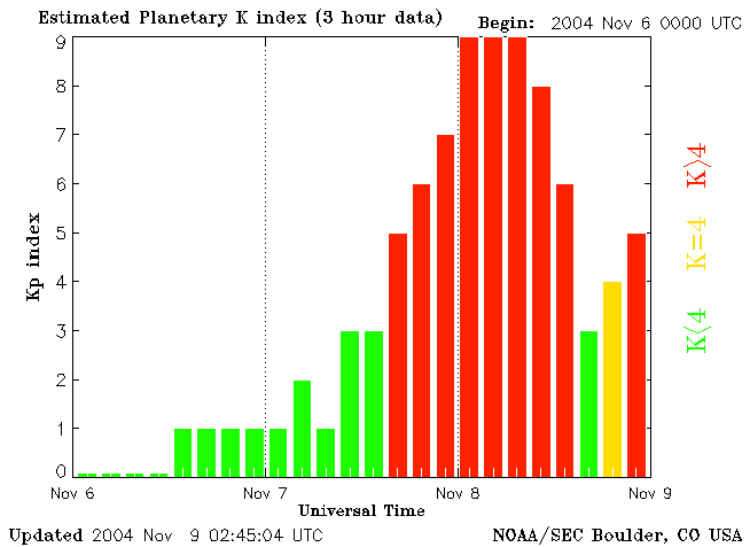


Fig. 13. KP Index at Nov. 8 in 2004, DOY 313 (Space Weather Live 2016).

frequency ratio was less than 1%.

Among the STEC analysis, days of excessively increased STEC difference were observed regardless of the diurnal, annual, and solar cycle. As shown in Fig. 12, the STEC difference was increased up to 50 TECU by the largest increase at DOY 313 in 2004. To determine the reason, the KP Index (Planetary K index) was checked and we found that there was a geomagnetic storm at DOY 313 in 2004. The KP Index shows a geomagnetic change in every three hour by averaging data observed from many geomagnetic observatories located between geomagnetic latitude 46-63 (Choi et al. 2005). The magnetic change is exhibited at the ground by the current around the earth due to charged particles emitted from the sun. The KP Index is classified into 10 grades from 0 to 9 according to disturbance intensity in order to express a level of disturbance in the magnetic

field due to the sun quantitatively. When strong solar storms reach the earth due to sunspot explosion and solar flare, it can cause significant disturbance in geomagnetic field. Six to Nine Grades indicate relatively severe geomagnetic storms and Zero to Three Grades indicate a relatively quiet state without geomagnetic storm. As shown in Fig. 12, days of excessively increased STEC difference were confirmed that they were due to the effect of the geomagnetic storms regardless of periodicity. Fig. 13 shows the KP Index of DOY 313 in 2004 (Space Weather Live 2016).

## 6. CONCLUSION

In this study, the variation pattern of the ionosphere and STEC difference between Busan and Sinuiju, which

is the longest baseline in the southeastern direction in the Korean Peninsula, were analyzed through GIM data for 12 years from 2003 to 2014. The variation in the ionosphere was affected by solar activities and STEC difference between Busan and Sinuiju was also much affected by solar activities. Due to the influence of the sun, diurnal, annual, and solar cycle variations occurred. The diurnal variation showed that as the ionosphere value was increased at 6-7 am when the sun arose, the STEC difference between Busan and Sinuiju also started to increase. The STEC difference was the largest at 13-14 pm and then started to decrease. The seasonal variation was characterized that the variation in the STEC was high in spring and autumn whereas it was low in summer and winter. The solar cycle variation revealed that the variation in the STEC increased up to 60 TECU during solar maximum and decreased up to 20 TECU during solar minimum. When days of excessively increased STEC difference were observed without showing periodicity due to geomagnetic storms caused by sunspot explosion and solar flare, we found via comparison of the KP Index that they were due to geomagnetic storms. The relative frequency where the STEC difference between Busan and Sinuiju was more than 10 TECU showed a similar cycle with that of the ionospheric variation. The relative frequency was up to 20% during solar maximum and less than 1% during solar minimum. Through the analysis on the long baseline STEC difference, periodicity of STEC difference between Busan and Sinuiju according to the diurnal, annual, and solar cycle was verified. We expect that this study result contribute to foundation research on algorithm development that can predict the ionospheric error during relative positioning of long baseline where the ionospheric variation and maximum analysis are deviated from the reference network.

## ACKNOWLEDGMENTS

This research was supported by “Land, Infrastructure and Transport Technology Commercialization Support Business” of Ministry of Land, Infrastructure and Transport of Korean government.

## REFERENCES

Choi, B.-K. 2009, Development of a Regional Ionosphere Model for Improving Geodetic Performance in the Middle Range Baseline, PhD Thesis, Department of Electronic Engineering, Graduate School, Chungnam

- National University, Daejeon, Korea
- Choi, K.-C., Cho, K.-S., Moon, Y.-J., Kim, K.-H. Lee, D.-Y., et al. 2005, Near real-time estimation of geomagnetic local K Index from gyeongju magnetometer, *JASS*, 22, 431-440. <http://dx.doi.org/10.5140/JASS.2005.22.4.431>
- Hofmann-Wellenhof, B., Lichtenegger, H., & Wasle, E. 2008, *GNSS: Global navigation satellite systems: GPS, GLONASS, Galileo & More* (NY: Springer)
- Kang, J.-M., Nim, Y.-B., Song, S.-H., & Park, J.-H. 1996, Analysis of Baseline Accuracy by GPS Relative Positioning, *Journal of Korean Society for Geospatial Information System*, 4, 15-22
- Kim, H.-I., Kim, J.-H., Kim, K.-T., Park, K.-D., & Kim, D.-S. 2012, Accuracy Evaluation of DGPS Service via Terrestrial Digital Multimedia Broadcasting, *Journal of Navigation and Port Research*, 36, 437-442. <http://dx.doi.org/10.5394/KINPR.2012.36.6.437>
- Klobuchar, J. A. 1987, Ionospheric time-delay algorithm for single-frequency GPS users, *IEEE Transactions on Aerospace and Electronics Systems*, AES, 23, 325-331. <http://dx.doi.org/10.1109/TAES.1987.310829>
- Lee, C.-M., Park, K.-D., & Lee, S.-U. 2010, Comparison of Real-Time Ionospheric Delay Correction Models for Single-Frequency GNSS Receivers: Klobuchar Model and NeQuick Model, *Journal of the Korean Society of Survey, Geodesy, Photogrammetry and Cartography*, 28, 413-420.
- Misra, P. & Enge, P. 2011, *Global positioning system: Signals, measurements, and performance*, Revised Second Edition (MA: Ganga-Jamuna Press)
- NASA Solar cycle prediction 2016, [Internet], cited 2016 March 2. available from: <http://solarscience.msfc.nasa.gov/predict.shtml>
- Rishbeth, H. 1972, Superrotation of the upper atmosphere, *Reviews of Geophysics*, 10, 799-819. <http://dx.doi.org/10.1029/RG010i003p00799>
- Schaer, S., Gurtner, W., & Felten, J. 1998, IONEX: The IONosphere Map Exchange Format Version 1, *Proceedings of the IGS Analysis Centers Workshop*, ESOC, Darmstadt, Germany, February 9-11, 1998
- Sohn, D.-H. 2015, Characteristics of rapid phase variations of GPS signals in the northern auroral zone, PhD Thesis, Department of Geoinformatic Engineering, Graduate School, Inha University, Incheon, Korea
- Space Weather Live, KP index 2016, [Internet], cited 2016 March 10, available from: <https://www.spaceweatherlive.com/en/archive/2004/11/08/kp>



**Woong-Jun Yoon** is a BS candidate in geoinformatic engineering from Inha University, Korea. He is currently at Inha University as a student. His research interests include ionosphere analysis.



**Kwan-Dong Park** received his Ph. D. degree from the Department of Aerospace Engineering and Engineering Mechanics at the University of Texas at Austin, and he is currently at Inha University as a professor. His research interests include DGNS/PPP-RTK algorithm development and GNSS geodesy.